

IV International Seminar on ORC Power Systems, ORC2017  
13-15 September 2017, Milano, Italy

# Thermodynamic potential of Rankine and flash cycles for waste heat recovery in a heavy duty Diesel engine

Jelmer Rijpkema<sup>a,\*</sup>, Karin Munch<sup>a</sup>, Sven B. Andersson<sup>a</sup>

<sup>a</sup>Chalmers University of Technology, Hörsalsvägen 7B, 41280 Göteborg, Sweden

---

## Abstract

In heavy duty Diesel engines more than 50% of the fuel energy is not converted to brake power, but is lost as heat. One promising way to recapture a portion of this heat and convert it to power is by using thermodynamic power cycles. Using the heavy duty Diesel engine as the waste heat source, this paper evaluates and compares the thermodynamic potential of different working fluids in four power cycles: the Rankine cycle (RC), the transcritical Rankine cycle (TRC), the trilateral flash cycle (TFC) and the single flash cycle (SFC). To establish the heat input into the cycle, operating conditions from an actual heavy duty Diesel engine are used as boundary conditions for the cycle heat source. A GT-Power model of the engine was previously developed and experimentally validated for the stationary points in the European Stationary Cycle (ESC). An energy analysis of this engine revealed that it has four heat sources with the potential for waste heat recovery: the charge air cooler (CAC), the coolant flow, the exhaust gas recirculation cooler (EGRC), and the exhaust flow. Using fixed heat input conditions determined by the selected engine operating mode, the TFC performed best for the CAC with a net power increase of around 2 kW, while the RC performed best for the coolant flow, with a net power increase of 5 kW. For the EGRC, ethanol performed especially well with both the RC and TRC, leading to an 8 kW net power increase. When using the exhaust as heat source, all four cycles provided a power output of around 5 kW with some variation depending on the working fluid. This study shows that for most cases, considering the different heat sources, the choice of cycle has a larger impact on the cycle performance than the choice of working fluid.

© 2017 The Authors. Published by Elsevier Ltd.

Peer-review under responsibility of the scientific committee of the IV International Seminar on ORC Power Systems.

**Keywords:** energy analysis; internal combustion engine; organic flash cycle; organic Rankine cycle; single flash cycle; transcritical Rankine cycle; trilateral flash cycle; waste heat recovery

---

## 1. Introduction

Ever increasing consumer demands for lower fuel consumption and more stringent legislation on emissions drive developments for continuous improvements in internal combustion engine efficiency. A promising way to increase engine efficiency and thus reduce CO<sub>2</sub> emissions is to use thermodynamic power cycles for waste heat recovery (WHR). The Rankine cycle, a well-established technology for WHR in stationary applications [1–3], also shows

---

\* Corresponding author. Tel.: +46-(0)31-772 50 37

E-mail address: [jelmer.rijpkema@chalmers.se](mailto:jelmer.rijpkema@chalmers.se)

promising efficiencies for the use in automotive applications [4,5]. A possible way to increase the thermal efficiency of the RC is to bring the working fluid to supercritical conditions in the transcritical Rankine cycle (TRC). This has the potential to improve the thermal match between the heat source and the cycle, albeit often at the expense of higher system pressures [5–7]. Another alternative is the trilateral flash cycle (TFC), where the pressurized fluid is heated to its saturation point and then expanded into the two-phase region. Since only liquid is heated, there are opportunities to improve the thermal match while simultaneously improving heat transfer and reducing pressure drop [8–10], leading to smaller heat exchangers, an important consideration for WHR in automotive applications. Finally, to address the main drawback of the TFC - the inefficient expansion of the wet mixture - the performance of an alternate flash cycle is investigated: the single flash cycle (SFC). Instead of expanding a wet mixture from the saturation point, the fluid is flashed to an intermediate pressure, the vapor and liquid are separated, and then only the vapor is expanded. This technology is already commonly used for electricity production from geothermal sources [11], and previously proposed for WHR in stationary applications under the name OFC [12]. It combines improved thermal matching with more efficient expansion, albeit with the possible disadvantage of reduced temperatures, pressures and mass flows as well as the need for an extra component in the form of a flash vessel.

This work evaluates and compares the thermodynamic potential of these four cycles using heat input conditions based on the heat sources available in a heavy duty Diesel engine. An energy analysis of different operating modes of the engine is performed and used to evaluate the potential heat sources in the engine, and one operating mode is selected for further analysis. The thermodynamic cycle models are simulated with a number of different working fluids, spanning a range of thermodynamic properties. Boundary conditions and cycle constraints have been chosen so that the thermodynamic potential of both low and high temperature heat sources can be evaluated and compared.

The paper aims to provide insight into the relative performance of the different thermodynamic cycles by making a direct comparison between the cycles. By considering all the relevant heat sources for the operating conditions in a heavy duty Diesel engine, including the low, intermediate and high temperature sources, it can be identified which combination of cycle and working fluid gives the highest thermodynamic potential for each heat source.

## Nomenclature

$h$	specific enthalpy, J/kg
$\dot{m}$	mass flow rate, kg/s
$M$	molecular mass, kg/kmol
$P$	pressure, Pa
$\dot{Q}$	heat transfer rate, W
$T$	temperature, K
$\bar{T}$	mean temperature, K
$\dot{W}$	power, W
$x$	vapor mass fraction
$\dot{X}$	exergy rate, W

### Greek symbols

$\eta$	efficiency
--------	------------

### Subscripts

0	reference state
con	condensation
cr	critical
ev	evaporation
eng	engine
exh	exhaust
exp	expander

### Subscripts (continued)

is	isentropic
pp	pinch point
sup	superheating
th	thermal
tot	total

### Abbreviations

CAC	charge air cooler
EATS	exhaust aftertreatment system
EGR	exhaust gas recirculation
EGRC	exhaust gas recirculation cooler
ESC	European stationary cycle
GWP	global warming potential
ODP	ozone depletion potential
OFC	organic flash cycle
ORC	organic Rankine cycle
RC	Rankine cycle
SFC	single flash cycle
TFC	trilateral flash cycle
TRC	transcritical Rankine cycle
WHR	waste heat recovery

## 2. Energy and exergy analysis of the engine

In a previous project at Chalmers University of Technology, a GT-Power [13] model of a heavy duty 12.8L Diesel engine was developed and experimentally validated for the operating modes in the European stationary cycle (ESC) [14], where the modes range from low to high engine speeds (A, B and C) and low to high engine loads (25, 50, 75 and 100). A schematic layout of the engine containing the components relevant for waste heat recovery is shown in Fig. 1. The inlet air, heated by compression, is cooled down in the charge air cooler (CAC) before it enters the cylinders. In the cylinders, fuel is added to the air and the mixture combusts, with some energy being lost to the coolant. Part of the exhaust gas leaving the cylinders is cooled in the exhaust gas recirculation cooler (EGRC) and mixed with air entering the cylinders. The other part of the mass flow is expanded in the turbocharger turbine and leaves the exhaust through the exhaust aftertreatment system (EATS), still containing a substantial amount of useful energy.

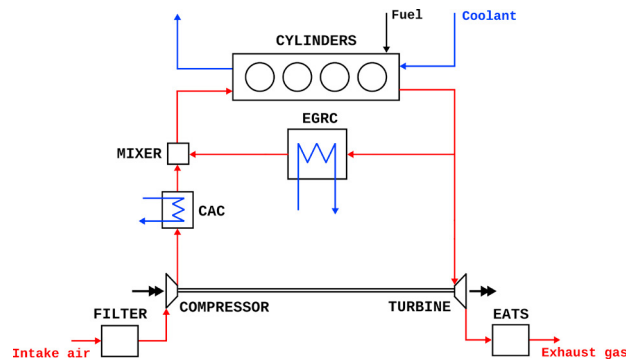


Fig. 1. Schematic layout of a heavy duty Diesel engine with a turbocharger and EGR.

Inside the engine four main sources of heat loss can be distinguished: the CAC, the coolant flow, the EGRC, and the exhaust flow. To determine if these losses are suitable for waste heat recovery, their temperatures, mass flows, and heat losses were determined. To evaluate the quality of the energy flows, they were converted to exergy flows using Eq. (1), which takes into account the mean temperature level ( $\bar{T}$ ) at which the energy is available [15].

$$\dot{X}_{\text{loss}} = \dot{Q}_{\text{loss}} \frac{\bar{T} - T_0}{\bar{T}} \quad (1)$$

## 3. Thermodynamic cycles

This paper considers four thermodynamic power cycles for waste heat recovery: the Rankine cycle, the transcritical Rankine cycle, the trilateral flash cycle, and the single flash cycle of which the schematic depictions are shown in Fig. 2. T-s diagrams belonging to these cycles are shown in Fig. 3. Both Rankine cycles involve the same sequence of steps:  $1 \rightarrow 2$ : compression,  $2 \rightarrow 3$ : heat addition,  $3 \rightarrow 4$ : expansion and  $4 \rightarrow 1$ : condensation. In the RC step  $2 \rightarrow 3$  involves evaporation of the fluid whereas the TRC operates with the fluid above its critical pressure and so no evaporation occurs. The TFC involves a similar sequence of steps, but the fluid is only heated until the saturation point (step  $2 \rightarrow 3$ ), and is then expanded into the two-phase region during step  $3 \rightarrow 4$ . The difficult wet expansion can be avoided by expanding to an intermediate pressure and then separating the vapor and liquid in a flash vessel as proposed in the SFC. In this case, steps  $1 \rightarrow 2$  and  $2 \rightarrow 3$  are the same as in the TFC, but are followed by  $3 \rightarrow 4$ : flash evaporation,  $4 \rightarrow 4'$ : vapor separation, and  $4' \rightarrow 5'$ : vapor expansion. The vapor is then mixed with the liquid from steps  $4 \rightarrow 4''$ : liquid separation and  $4'' \rightarrow 5''$ : liquid throttling. The mixture of liquid and vapor at low pressure is condensed in step  $6 \rightarrow 1$ .

Table 1 shows the reference and boundary conditions imposed in the cycle simulations. Previously reported efficiencies range from 0.65–0.90 for the pump and 0.70–0.85 for the expander [2–5,7,8,10,12], and from 0.60–0.85 for wet expansion, either obtained in experiments [16] or assumed in simulations [8–10,17]. Considering that this study evaluates the thermodynamic potential, relatively high efficiencies for the pump (0.80) and expander (0.85) have been selected. To account for the unfavorable aspects of wet expansion, a value of 0.60 was set for the TFC expander.

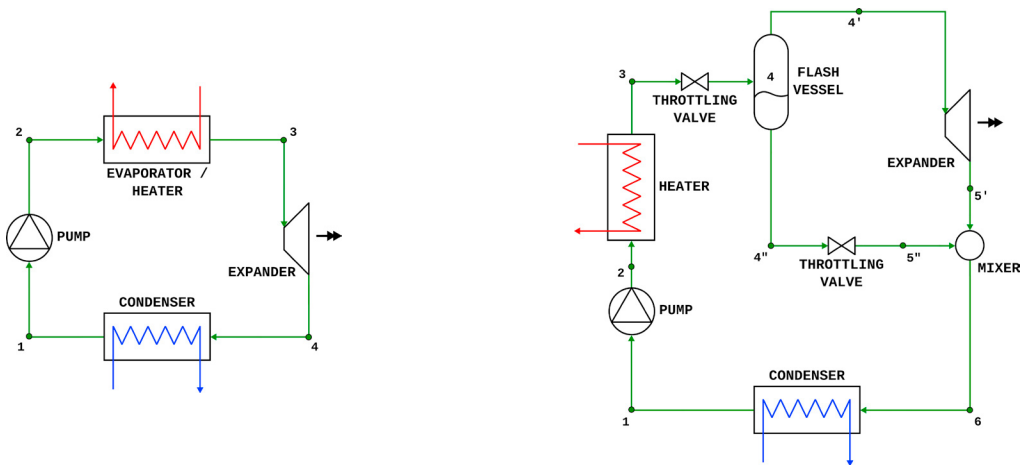


Fig. 2. Schematic depictions of the Rankine, transcritical Rankine and trilateral flash cycles (left) and the single flash cycle (right).

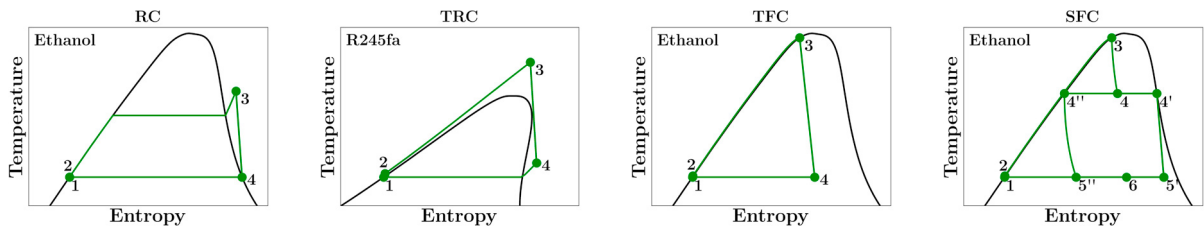


Fig. 3. T-s diagrams for the Rankine cycle (left), the transcritical Rankine cycle (middle left), the trilateral flash cycle (middle right) and the single flash cycle (right) for different working fluids and the same heat source.

A number of practical limits were imposed as constraints, shown in Table 1. For all cycles except the TRC, a maximum pressure limit of  $0.9 \cdot P_{cr}$  was set to avoid instabilities near the critical point. An upper limit for the pressure is difficult to obtain, but a value of 60 bar was previously reported [5]. To account for future developments, the maximum pressure was set to 100 bar in this work. Excessive superheating of the fluid should be avoided because of the unfavorable heat transfer coefficients and large volume flows associated with vapor flow. Therefore, for both the inlet of the condenser and the outlet of the evaporator, a maximum superheating temperature difference of 20 K was imposed. Finally, because expanders, and especially turbine expanders, are sensitive to two-phase flow during expansion, the upper limit for the vapor fraction at the end of expansion was set to 0.85 for all cycles except the TFC.

A steady-state model for each cycle was developed in the *Modelica* [18] language. Simulations were performed using the solvers available in *Dymola* [19] coupled to *Python* code [20] for pre- and post-processing. A number of assumptions were employed in this study: no pressure losses in the system; no heat losses to the environment for all components, including the heat exchangers; changes in potential and kinetic energy were neglected; isenthalpic expansion in the throttling valves; perfect mixing and separation of the working fluid.

Table 1. Reference conditions, boundary conditions and constraints.

Reference and boundary conditions			Constraints			
Ambient temperature	$T_0$	25 °C	High pressure	Max.	$P_{max}$	100 bar
Ambient pressure	$P_0$	1.013 bar				$0.9 \cdot P_{cr}^\dagger$ bar
Condensation temperature	$T_{con}$	40 °C	Superheating evaporation	Max.	$\Delta T_{sup,ev}$	20 K
Pump isentropic efficiency	$\eta_{is,pump}$	0.80	Superheating condensation	Max.	$\Delta T_{sup,con}$	20 K
Expander isentropic efficiency	$\eta_{is,exp}$	0.85	Pinch point temperature difference	Min.	$\Delta T_{pp}$	10 K
		0.60*	Expander vapor quality out	Min.	$x_{exp,out}$	0.85‡
Pump vapor quality in	$x_{pump,in}$	0				

\*Only applicable to TFC, †not applicable to TRC, ‡not applicable to TFC

#### 4. Working fluids

Four working fluids, shown in Table 2, were selected for consideration to cover a range of properties and based on their performance for medium and low temperature heat sources [1,3,9]. While a low GWP alternative to R245fa with similar thermodynamic properties and performance is available in the form of R1233zd [21], R245fa was selected because it has been used extensively in many other studies [1,2,7,10]. The fluid properties used in the *Modelica* [18] models were obtained by coupling the models to the *CoolProp* database [22] using the *ExternalMedia* library [23].

Table 2. Thermodynamic and environmental properties of the working fluids.

Fluid	$M$ [kg/kmol]	$T_{cr}$ [°C]	$P_{cr}$ [bar]	$P_{40^\circ\text{C}}$ [bar]	$T_{1\text{atm}}$ [°C]	Type	GWP <sub>100</sub>	ODP	Refs.
Cyclopentane	70.13	238.6	45.7	0.74	49.3	Isen.	0	0	[24,25]
Ethanol	46.07	240.2	62.7	0.18	78.4	Wet	0	0	[5,25]
R245fa	134.05	154.0	36.5	2.50	15.1	Dry	858	0	[25,26]
Water	18.02	374.0	220.1	0.07	100.0	Wet	0	0	[5,25]

#### 5. Results

Previously, four potential waste heat sources were identified: the CAC, the coolant flow, the EGRC, and the exhaust flow. The left-hand side of Fig. 4 shows the inlet temperature and mass flow ranges for these sources, obtained from the GT-Power model for the twelve operating modes in the ESC. Since the model included only heat losses to the coolant with no information regarding the mass flows or temperatures, the figure does not show coolant data. The waste heat sources in the engine operate at different temperatures, making it difficult to select a single working fluid that is suitable for all of them. The model data were also used to calculate the heat and exergy loss ranges shown on the right-hand side of Fig. 4, in which the losses for each source are reported as percentages of the total loss. The figure indicates that each source contributes significantly to the total heat loss. However, based on the temperatures at which the energy is available, shown by the exergy losses, the exhaust flow and EGRC clearly contribute most. The label *Other* represents other heat losses in the engine, primarily heat losses in the exhaust piping and the EATS.

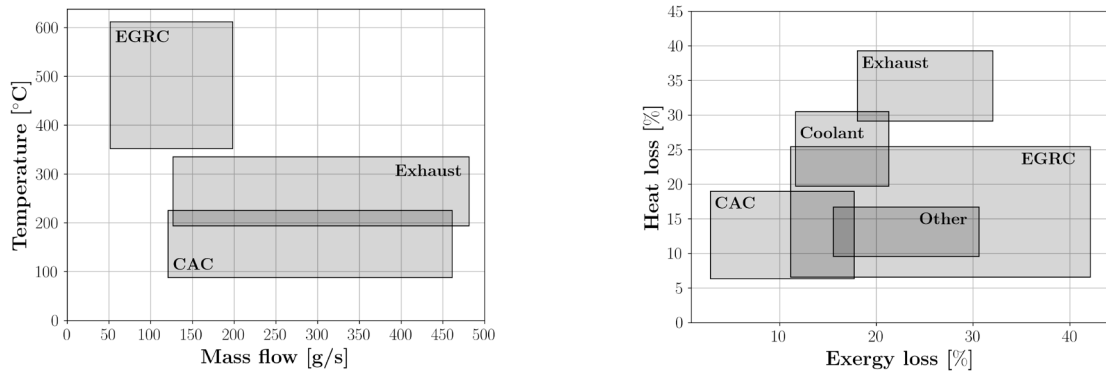


Fig. 4. Ranges of mass flows and inlet temperatures (left) and heat and exergy losses (right) for all operating modes in the ESC obtained from the GT-Power model. The exhaust losses are calculated with reference to the environment:  $\dot{Q}_{\text{loss,exh}} = \dot{m}_{\text{exh}}(h_{\text{exh}} - h_0)$ . All the losses are expressed as percentages of the total losses.

The energy analysis indicated that the selected sources all have significant heat and exergy losses, so all four were included in the cycle analysis as a potential waste heat source. Of the twelve operating modes, the low speed, medium load operating mode (A50) was selected for further evaluation because it is one of the dominant modes in a typical long haul duty cycle [4]. Table 3 shows the operating conditions chosen for each waste heat source. Some of these values (shown in italics) were modified from those used in the model to provide valid input values for the cycle simulations. The CAC outlet temperature was increased because the model value for this parameter was below the condensation temperature. The exhaust temperature after WHR was set to 100 °C and the coolant conditions were set to representative values for the chosen operating mode.

Table 3. Conditions of waste heat sources for the selected operating mode. Values shown in italics differ from the corresponding GT-power model values.

Source	Fluid	$P$ [bar]	$\dot{m}$ [g/s]	$T_{in}$ [°C]	$T_{out}$ [°C]	$\dot{Q}_{loss}$ [kW]	$\dot{X}_{loss}$ [kW]
CAC	Air	2.47	231	152	60	21.7	4.6
Coolant	Water	<i>1.013</i>	<i>4317</i>	93	90	54.4	9.9
EGRC	Exhaust gas	2.49	73	472	95	30.6	<i>13.6</i>
Exhaust	Exhaust gas	1.013	239	251	100	33.2	<i>11.0</i>

The conditions given in Table 3, constant for all four cycles, as well as the boundary conditions and constraints presented in Table 1, result in the thermal efficiencies and corresponding net power output values ( $\dot{W}_{net}$ ) presented in Fig. 5 and Fig. 6. Unsurprisingly, waste heat sources with higher temperatures yielded higher thermal efficiencies. Because of the constant condensation temperature, higher source temperatures allow for higher cycle temperature and pressure differences, giving better performance. The variation between the different cycles and fluids for each heat source then depends on how well the cycle temperature profile matches the source temperature profile. This is particularly visible for the coolant flow, where the RC outperforms all other cycles, although the temperatures at the expander inlet are similar. The small temperature drop in the coolant flow leads to a source temperature profile that is nearly horizontal, which matches well with the evaporation phase in the RC as shown in Fig. 7.

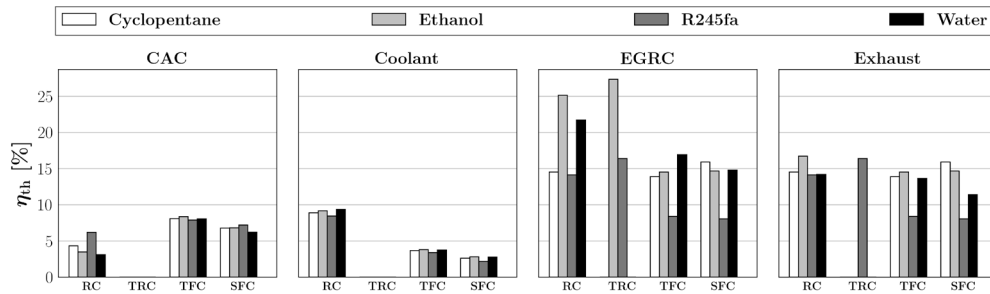


Fig. 5. Thermal efficiencies ( $\eta_{th} = \dot{W}_{net} / \dot{Q}_{loss}$ ) for each combination of cycle and heat source.

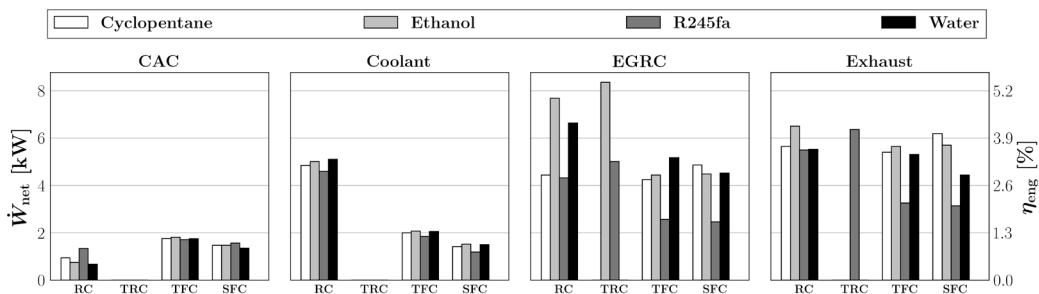


Fig. 6. Net produced power in kW ( $\dot{W}_{net} = \dot{W}_{exp} - \dot{W}_{pump}$ ) and the ratio of net produced power to engine power ( $\eta_{eng} = \dot{W}_{net} / \dot{W}_{eng}$ ) for each combination of cycle and heat source.

Additionally, the RC performs well with the EGRC as the heat source, especially with ethanol and water as the working fluids. In most EGRC cases, performance is limited by the maximum pressure, except for the *EGRC-Water* case where the pinch point and evaporation superheating are the limiting factors, shown in Fig. 7. When using the CAC as the heat source, it is difficult to achieve a good match with the RC because the low source outlet temperature and pinch point limitation prevent the RC from achieving high pressures. In this case, the TFC offers a better match, also shown in Fig. 7. In general, the TFC provides good efficiencies for every heat source even though the isentropic efficiency of the expander is lower. The SFC provides similar efficiencies to the TFC although it is operating at reduced temperatures and pressures due to flashing. Lower temperatures and pressures are not necessarily a disadvantage because it also means reduced expansion ratios, a possible benefit for expansion. With the exhaust flow as the heat source, the efficiencies of the TFC and SFC match those of the RC and TRC, offering power outputs of around 5 kW.

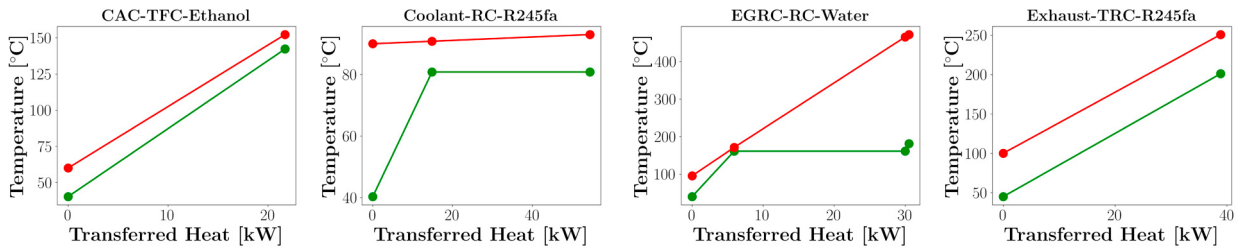


Fig. 7. Q-T diagrams of the cases CAC-TFC-Ethanol (left), Coolant-RC-R245fa (middle left), EGRC-RC-Water (middle right) and Exhaust-TRC-R245fa (right). The top (red) line shows the source temperatures and the bottom (green) line shows the cycle temperatures.

The TRC yielded the best overall performance, generating over 8 kW for the *EGRC-Ethanol* case. Since this cycle allows for good matching with the heat source (see Fig. 7), has good expander efficiency, and was only limited by the maximum pressure of 100 bar, it achieved good performance in all three cases for which it was evaluated. Although supercritical conditions were also achieved in the *Exhaust-Ethanol*, *EGRC-Cyclopentane* and *Exhaust-Cyclopentane* cases, these cases were not taken into account because the expansion led into the two-phase region. In the case of water, the maximum pressure was below the critical pressure, thus never leading to critical conditions for this fluid.

## 6. Discussion

The working fluids in this study were selected on the basis of their range of properties and their promising performance for similar temperature levels in other studies. However, this selection of working fluids is not exhaustive and will, therefore, be extended in future studies to provide a more complete evaluation of the thermodynamic potential.

Relevant to note is the effect of the choice of boundary conditions and constraints on the results. Especially important is the condensation temperature, which was set to 40 °C so that the low temperature heat sources could be included, enabling a fair comparison of the thermodynamic potential for all heat sources. However, this meant ignoring two important practical considerations. Firstly, the temperature at which the heat is rejected is lowered to 40 °C, thereby drastically reducing the temperature difference between the ambient temperature and the heat rejection temperature, making it more difficult to reject the heat. Secondly, in the case of ethanol and water, the low condensation temperature leads to low saturation pressures, meaning large specific fluid volumes. This can lead to very high and unrealistic expansion ratios as well as high volume flows at the expander outlet, which is related to the pressure drop and thus affects condenser sizing. Also, the expander efficiencies for the cycles directly impact the resulting power output. Variation of these efficiencies and their impact is interesting for future studies, especially since a different value for the TFC expander was used. The maximum pressure limit directly affects the results as well, altering this limit can have a significant impact on the cycle performance. Including all relevant input parameters in a sensitivity analysis will provide a wider perspective on the potential for each combination of cycle, fluid and heat source.

Furthermore, heat losses and pressure drop in the heat exchangers have been ignored, although they can have a significant impact. Related to this are the constraints on the superheating temperature difference, which have been set to avoid excessive superheating. Implementation of heat transfer and pressure drop relations would allow evaluation of the effect of heat transfer, heat losses and pressure losses on cycle performance and heat exchanger sizing.

## 7. Conclusions

This paper compares four different thermodynamic power cycles, four working fluids and four waste heat sources available in a heavy duty Diesel engine. Its goal is to show the thermodynamic potential for each combination of cycle, fluid and heat source under the boundary conditions and constraints listed in Table 1. An energy analysis of the engine using data from a validated GT-Power model revealed that all the selected heat sources - the CAC, the coolant flow, the EGRC and the exhaust flow - have the potential for waste heat recovery. The input conditions for the simulations were based on the low speed, medium load ESC operating mode (A50) and were held constant.

Given these input conditions, the TFC and SFC offered the best performance with the CAC as the heat source, regardless of the selected working fluid. Because of good thermal matching, the RC performed especially well with

the coolant flow as the heat source, achieving power increases up to 5 kW, again also almost independently of the working fluid. Ethanol was the best performing working fluid with the EGRC as the heat source, offering peak power around 8 kW in both the RC and TRC. All cycles achieved similar performance when using the exhaust flow as the heat source, with peak power production of around 5 kW depending on the working fluid. For the high temperature heat sources, R245fa performed significantly worse than the other selected working fluids. Considering the working fluids and constraints employed in this study, the results showed that the choice of cycle had the largest impact on the performance, while in most cases the working fluids performed comparably. This can be attributed to the thermal matching: a better thermal match leads to an increased high temperature, giving better thermodynamic performance.

Even though a relatively low expander efficiency was assumed in the TFC simulations, this cycle offered similar performance to the RC and TRC, especially for the exhaust flow. In addition, even with reduced mass flows, temperatures and pressures, the SFC offered comparable performance while avoiding wet expansion, although it necessitates an extra component. Importantly, both SFC and TFC have liquid on both sides of the high temperature heat exchanger, allowing for a reduced area. Consequently, these cycles are particularly interesting for automotive waste heat recovery.

## References

- [1] Colonna, P., Casati, E., Trapp, C., Mathijssen, T., Larjola, J., Turunen-Saaresti, T., et al. Organic Rankine Cycle Power Systems: From the Concept to Current Technology, Applications, and an Outlook to the Future. *Journal of Engineering for Gas Turbines and Power* 2015;137.
- [2] Macián, V., Serrano, J.R., Dolz, V., Sánchez, J.. Methodology to design a bottoming Rankine cycle, as a waste energy recovering system in vehicles. *Study in a HDD engine. Applied Energy* 2013;104.
- [3] Quoilin, S., Declaye, S., Tchanche, B.F., Lemort, V.. Thermo-economic optimization of waste heat recovery Organic Rankine Cycles. *Applied Thermal Engineering* 2011;31.
- [4] Edwards, S., Eitel, J., Pantow, E., Geskes, P., Lutz, R., Tepas, J.. Waste Heat Recovery: The Next Challenge for Commercial Vehicle Thermomanagement. *SAE International Journal of Commercial Vehicles* 2012;5.
- [5] Latz, G., Andersson, S., Munch, K.. Comparison of Working Fluids in Both Subcritical and Supercritical Rankine Cycles for Waste-Heat Recovery Systems in Heavy-Duty Vehicles. In: *SAE Technical Paper* 2012-01-1200. 2012..
- [6] Chen, H., Goswami, D.Y., Stefanakos, E.K.. A review of thermodynamic cycles and working fluids for the conversion of low-grade heat. *Renewable and Sustainable Energy Reviews* 2010;14.
- [7] Schuster, A., Karellas, S., Aumann, R.. Efficiency optimization potential in supercritical Organic Rankine Cycles. *Energy* 2010;35.
- [8] Fischer, J.. Comparison of trilateral cycles and organic Rankine cycles. *Energy* 2011;36.
- [9] Steffen, M., Löffler, M., Schaber, K.. Efficiency of a new Triangle Cycle with flash evaporation in a piston engine. *Energy* 2013;57.
- [10] Yari, M., Mehr, A.S., Zare, V., Mahmoudi, S.M.S., Rosen, M.A.. Exergoeconomic comparison of TLC (trilateral Rankine cycle), ORC (organic Rankine cycle) and Kalina cycle using a low grade heat source. *Energy* 2015;83.
- [11] DiPippo, R.. *Geothermal Power Plants - Principles, Applications, Case Studies and Environmental Impact* (4th Edition). Elsevier; 2016.
- [12] Ho, T., Mao, S.S., Greif, R.. Comparison of the Organic Flash Cycle (OFC) to other advanced vapor cycles for intermediate and high temperature waste heat reclamation and solar thermal energy. *Energy* 2012;42.
- [13] Gamma Technologies, Inc. *GT-Suite, Version 7.5.0 Modified Build 1*; 2014.
- [14] Latz, G., Andersson, S., Munch, K.. Selecting an Expansion Machine for Vehicle Waste-Heat Recovery Systems Based on the Rankine Cycle. *SAE International* 2013;1.
- [15] Szargut, J., Morris, D., Steward, F.. *Exergy analysis of thermal, chemical, and metallurgical processes*. Hemisphere; 1988.
- [16] Smith, I., Stosic, N., Kovacevic, A.. Power recovery from low cost two-phase expanders. In: *Transactions-Geothermal Resources Council*. 2001, p. 601–606.
- [17] Zamfirescu, C., Dincer, I.. Thermodynamic analysis of a novel ammonia-water trilateral Rankine cycle. *Thermochimica Acta* 2008;477.
- [18] Modelica Association. *Modelica language specification, Version 3.3*; 2012.
- [19] Dassault Systemes. *Dymola, Version 2016 FD01*; 2016.
- [20] Python Software Foundation. *Python language reference, Version 2.7.13*; 2017.
- [21] Eyerer, S., Wieland, C., Vandersickel, A., Spliethoff, H.. Experimental study of an ORC (Organic Rankine Cycle) and analysis of R1233zd-E as a drop-in replacement for R245fa for low temperature heat utilization. *Energy* 2016;103.
- [22] Bell, I.H., Wronski, J., Quoilin, S., Lemort, V.. Pure and pseudo-pure fluid thermophysical property evaluation and the open-source thermophysical property library coolprop. *Industrial & Engineering Chemistry Research* 2014;53.
- [23] Casella, F., Richter, C.. ExternalMedia: A Library for Easy Re-Use of External Fluid Property Code in Modelica. In: *Proceedings 6th International Modelica Conference*. 2008, p. 157–161.
- [24] Braimakis, K., Leontaritis, A.D., Preißinger, M., Karellas, S., Brüggeman, D., Panopoulos, K.. Thermodynamic investigation of waste heat recovery with subcritical and supercritical low-temperature Organic Rankine Cycle based on natural refrigerants and their binary mixtures. In: *Proceedings of ECOS*. 2014, p. 611–636.
- [25] Lemmon, E.W., Huber, M.L., McLinden, M.O.. *NIST Standard Reference Database 23: Reference Fluid Thermodynamic and Transport Properties - REFPROP; 9.1 ed.* National Institute of Standards and Technology, Standard Reference Data Program; Gaithersburg; 2013.
- [26] IPCC, . *Climate Change 2013: The Physical Science Basis. Contribution of Working Group I to the Fifth Assessment Report of the Intergovernmental Panel on Climate Change*. Cambridge University Press; 2013.